



Anisotropic magnetic behaviors of monoclinic $\text{Li}_3\text{Fe}_2(\text{PO}_4)_3$



Zhangzhen He^{a,*}, Wenbin Guo^a, Wendan Cheng^a, Mitsuru Itoh^b

^a State Key Laboratory of Structural Chemistry, Fujian Institute of Research on the Structure of Matter, Chinese Academy of Sciences, Fuzhou, Fujian 350002, China

^b Materials and Structures Laboratory, Tokyo Institute of Technology, 4259 Nagatsuta, Midori, Yokohama 226-8503, Japan

ARTICLE INFO

Article history:

Received 22 November 2013

Received in revised form

26 March 2014

Accepted 1 April 2014

Available online 12 April 2014

Keywords:

$\text{Li}_3\text{Fe}_2(\text{PO}_4)_3$

Battery materials

Weak ferrimagnetism

Magnetic anisotropy

ABSTRACT

Large sized $\alpha\text{-Li}_3\text{Fe}_2(\text{PO}_4)_3$ single crystals with high quality are successfully grown by a flux method. Magnetic behaviors of the grown crystals are investigated by means of magnetic susceptibility, magnetization, and heat capacity measurements along different directions. The results confirm that $\alpha\text{-Li}_3\text{Fe}_2(\text{PO}_4)_3$ exhibits weak ferrimagnetic behaviors at low temperature, which are in good agreement with those reported previously. However magnetic anisotropy is confirmed for the first time, suggesting that the *c*-axis is the likely magnetic easy axis and the *a*-axis is the magnetic hard one. Two anomalies are clearly observed in magnetic susceptibility along the *a*-axis and heat capacity data at zero field, suggesting the appearance of two successive magnetic transitions at ~ 26 and ~ 22 K in the system.

© 2014 Elsevier Inc. All rights reserved.

1. Introduction

Phosphates with a three-dimensional polyanionic structure have attracted great interest in the past decades, since the discovery of fast ion transport properties of nasicon systems [1]. One of the most widely investigated nasicon phosphates is $\text{Li}_3\text{M}_2(\text{PO}_4)_3$ ($M = \text{Cr}, \text{Sc}, \text{In}, \text{Fe}$), which could be used as lithium solid-state electrolytes [2,3]. Among them, considerable attention has however been focused on $\text{Li}_3\text{Fe}_2(\text{PO}_4)_3$, a compound that is considered as a potential insertion-electrode material in lithium-polymer batteries, due to its favorable redox properties, good ionic conductivity, and low cost [4]. $\text{Li}_3\text{Fe}_2(\text{PO}_4)_3$ has two crystallographic forms of high-temperature monoclinic alpha-phase ($P2_1/n$) and low-temperature rhombohedral beta-phase ($R\bar{3}$), in which the structural transition occurs at 570°C [5–7]. The two distinct forms can be prepared by depending on different syntheses methods, in which the monoclinic form is obtained using a high-temperature solid state reaction while the rhombohedral one is obtained by ion exchange from $\text{Na}_3\text{Fe}_2(\text{PO}_4)_3$ in LiNO_3 aqueous solution [7].

Due to the presence of magnetic Fe^{3+} ions in the structural framework of $\text{Li}_3\text{Fe}_2(\text{PO}_4)_3$, the study of magnetic structure and properties has been an important issue for experimental and theoretical investigations in order to clarify the nature of desirable potential versus Li/Li^+ , corresponding to the reduction/oxidation of $\text{Fe}^{3+}/\text{Fe}^{2+}$. It was found that both α - and β - $\text{Li}_3\text{Fe}_2(\text{PO}_4)_3$ exhibit a quite similar magnetic structure, showing a weak ferrimagnetic

ordering at 29 and 27 K, respectively [8–14]. As shown in Fig. 1, the crystal structure of $\alpha\text{-Li}_3\text{Fe}_2(\text{PO}_4)_3$ exhibits a three-dimensional framework built by slightly distorted FeO_6 octahedra and PO_4 tetrahedra with corner-sharing oxygen atoms. Each FeO_6 octahedron is surrounded by six PO_4 tetrahedra, while each PO_4 tetrahedron is linked to four FeO_6 octahedra, forming a three-dimensional mixed heterogeneous network $\{\text{Fe}_2(\text{PO}_4)_3\}_\infty$, in which lithium ions are located inside. All of the interaction exchanges between Fe^{3+} ions are found through a more complicated Fe-O-P-O-Fe path. The weak ferrimagnetic behaviors observed at low-temperature are suggested to originate from an incomplete compensation of the antiparallel magnetic moments of two different crystallographic sites of Fe(1) and Fe(2) in the structural framework of $\alpha\text{-Li}_3\text{Fe}_2(\text{PO}_4)_3$.

Although magnetic behaviors of $\text{Li}_3\text{Fe}_2(\text{PO}_4)_3$ have been investigated intensively, almost all previous studies were carried out on polycrystalline samples [8–14]. It is well known that a single crystal sample is necessary to identify the nature of magnetic properties of materials, since magnetic anisotropic behaviors can be investigated in detail. This leads us to obtain a large-sized single crystal sample for magnetic measurements. Herein, we report on the successful growth of $\alpha\text{-Li}_3\text{Fe}_2(\text{PO}_4)_3$ single crystals. Further, the magnetic properties of $\alpha\text{-Li}_3\text{Fe}_2(\text{PO}_4)_3$ are investigated by means of magnetic and heat capacity measurements along different crystallographic directions of the grown crystals.

2. Experimental section

A mixture of high purity reagents of Li_2CO_3 (3 N, 7.4 g), Fe_2O_3 (3 N, 32 g), $\text{NH}_4\text{H}_2\text{PO}_4$ (3 N, 46 g), and LiF (3 N, 5.2 g) was ground

* Corresponding author. Tel./fax: +86 591 83792649.

E-mail addresses: hcz1988@hotmail.com, hezz@fjirsm.ac.cn (Z. He).

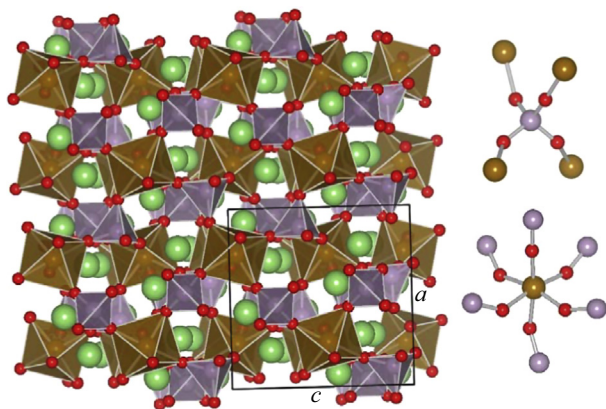


Fig. 1. The structure of $\alpha\text{-Li}_3\text{Fe}_2(\text{PO}_4)_3$ viewed along the b -axis, in which octahedra, tetrahedra, brown, pink, and red circles represent FeO_6 , PO_4 , Fe, P, and O, respectively. Oxygen-coordination environments for Fe and P are also seen. (For interpretation of the references to color in this figure legend, the reader is referred to the web version of this article.)



Fig. 2. Single crystals of $\alpha\text{-Li}_3\text{Fe}_2(\text{PO}_4)_3$ obtained by a flux method.

carefully and homogenized thoroughly with ethanol (99%) in an agate mortar. The mixture was packed into an alumina crucible ($\phi 42 \times 50 \text{ mm}^3$) capped with a cover using Al_2O_3 cement (C-989, Cotronics Corp.) and then the closed crucible was put into an electric furnace. The furnace was heated up to 1050°C and kept at 1050°C for 10 h to complete melting homogeneously. The furnace was slowly cooled down to 700°C at a rate of 1°C/h while keeping at a constant temperature several times, and then cooled down to room temperature at a rate of about 100°C/h . With this procedure, some yellowish-brown crystals with a size of $2 \times 2 \times 6 \text{ mm}^3$ (Fig. 2) were obtained by mechanical separation from the crucible.

The quality of grown crystals was confirmed by X-ray powder diffraction (XRD) data which was collected at room temperature in the range $2\theta = 10\text{--}80^\circ$ with a scan step width of 0.02° and a fixed counting time of 4 s using an MXP21AHF (Mac Science) powder diffractometer with graphite monochromatized $\text{CuK}\alpha$ radiation. Elemental analysis of the crystals was performed on a field emission scanning electron microscope (FESEM, JSM6700F) equipped with an energy dispersive X-ray spectroscope (EDS, Oxford INCA). Directions of the surface of crystals were determined using a Bruker SMART three-circle diffractometer equipped with a CCD area detector. Magnetic and heat capacity measurements were performed using a commercial Quantum Design Physical Property Measurement System (PPMS); dc magnetic susceptibility was measured at 0.1 T from 300 to 2 K and ac susceptibility was measured at an amplitude of 10 Oe and different

frequencies from 2 to 100 K. Magnetization was measured at 2 K in applied field from 0 to 9 T. Heat capacity data was measured at different fields by a relaxation method.

3. Results and discussion

Fig. 3 shows a typical powered XRD pattern obtained from the crushed crystals of $\alpha\text{-Li}_3\text{Fe}_2(\text{PO}_4)_3$. On indexing the Bragg reflections, it was found that all peaks of the XRD pattern can be indexed with the monoclinic system and identified to diffraction peaks from $\alpha\text{-Li}_3\text{Fe}_2(\text{PO}_4)_3$ (Ref.: ICSD Code 62244). No impurity phases were detected. The inset of Fig. 3 shows a typical EDS spectrum of $\alpha\text{-Li}_3\text{Fe}_2(\text{PO}_4)_3$. Other metal elements were not confirmed except for Fe and P, agreeing with the component of the titled compound, while Li element was too light to be detected. These results may show that the grown crystals are $\alpha\text{-Li}_3\text{Fe}_2(\text{PO}_4)_3$ and have good quality.

Fig. 4 shows the temperature dependence of magnetic susceptibilities (χ_a , χ_b , and χ_c) obtained at magnetic field of 0.1 T along the crystallographic a -, b -, and c -axes. Susceptibilities increase with decreasing temperature, while rapid increases are seen at around 30 K, showing the onset of magnetic ordering. A typical Curie–Weiss behavior is observed above 30 K, giving the Curie constant $C = 9.81(6) \text{ emu K/mol}$ and Weiss constant $\theta = -81.6(6) \text{ K}$. The effective magnetic moment (μ_{eff}) is calculated to be $6.26(6) \mu_B$, which is larger than the value $5.916 \mu_B$ for $S = 5/2$ with a g factor of 2, suggesting magnetic anisotropy in the system. We note that the saturation in susceptibility can be seen at low temperature, suggesting the development of ferromagnetic correlation. Such ferromagnetic correlation and negative Weiss constant indicate that the ground state of $\alpha\text{-Li}_3\text{Fe}_2(\text{PO}_4)_3$ is likely to be weakly ferrimagnetic. In addition, deviation of susceptibilities along a -, b -, and c -axes is seen below 30 K, supporting magnetic anisotropy in the system. Further, we note different magnitudes of the susceptibilities with $\chi_c > \chi_b > \chi_a$, showing that the c -axis is the likely magnetic easy axis and the a -axis is the magnetic hard one.

Compared to the b - and c -axes, different magnetic behaviors are found along the magnetic hard a -axis. As shown in Fig. 5(a), a rapid upturn is seen at around 26 K, while an anomaly is observed at $\sim 22 \text{ K}$. These findings indicate two successive magnetic transitions along the a -axis; ac susceptibilities obtained at

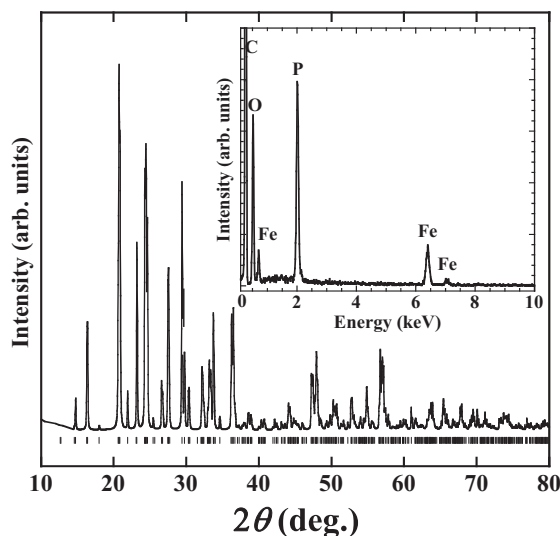


Fig. 3. The powdered XRD pattern for $\alpha\text{-Li}_3\text{Fe}_2(\text{PO}_4)_3$ using crushed crystals. The Bragg reflections are indicated by vertical marks. The inset shows a typical EDS spectrum acquired from $\alpha\text{-Li}_3\text{Fe}_2(\text{PO}_4)_3$ crystals coated with carbon.

Download English Version:

<https://daneshyari.com/en/article/7759101>

Download Persian Version:

<https://daneshyari.com/article/7759101>

[Daneshyari.com](https://daneshyari.com)